




# Epigenetic priming sensitizes gastric cancer cells to irinotecan and cisplatin by restoring multiple pathways

Hiroshi Moro<sup>1,2</sup> · Naoko Hattori<sup>1</sup> · Yoshiaki Nakamura<sup>1,3</sup> · Kana Kimura<sup>1</sup> · Toshio Imai<sup>4</sup> · Masahiro Maeda<sup>1</sup> · Masakazu Yashiro<sup>5</sup> · Toshikazu Ushijima<sup>1,2</sup> 

Received: 27 June 2019 / Accepted: 2 September 2019 / Published online: 25 September 2019  
© The International Gastric Cancer Association and The Japanese Gastric Cancer Association 2019

## Abstract

**Background** Gastric cancer is heavily influenced by aberrant DNA methylation that alters multiple cancer-related pathways, and may respond to DNA demethylating agents, such as 5-aza-2'-deoxycytidine (5-aza-dC). Here, we aimed to analyze whether 5-aza-dC can sensitize gastric cancer cells to clinically used cytotoxic drugs.

**Methods** Ten gastric cancer cell lines were treated with 5-aza-dC for 72 h and their growth was analyzed by conducting WST assay. In vivo effect of the drugs was analyzed using xenografts of OCUM-2 M/SN38 cells. Genome-wide expression and DNA methylation analyses were conducted using microarrays, and biological functions were identified through ingenuity pathway analysis.

**Results** The cell lines most resistant to SN38 (an active metabolite of irinotecan), CDDP, PTX, and 5-FU, were identified. 5-Aza-dC pre-treatment of the resistant cell lines decreased the IC<sub>50</sub> values for SN38 (TMK1, 226.4 nM to 32.91 nM; 44As3, 128.2 nM to 19.32 nM; OCUM2 M/SN38, 74.43 nM to 16.47 nM) and CDDP (TMK1, 5.05 μM to 2.26 μM; OCUM2 M, 10.79 μM to 2.77 μM), but not PTX and 5-FU. The reactivation of apoptosis-related genes, such as *RUNX3*, *PYCARD*, *TNF*, *FAS*, and *FASLG*, was induced by pre-treatment with 5-aza-dC, and the DNA demethylation of promoter CpG islands of *RUNX3* and *PYCARD* was confirmed. In a xenograft model with OCUM2 M/SN38, treatment with 5-aza-dC before irinotecan showed markedly enhanced tumor suppression.

**Conclusion** Epigenetic priming with 5-aza-dC can improve the sensitivity of gastric cancer cells to SN38 and CDDP.

**Keywords** DNA methylation · Resistance · Decitabine · Irinotecan · Cisplatin

**Electronic supplementary material** The online version of this article (<https://doi.org/10.1007/s10120-019-01010-1>) contains supplementary material, which is available to authorized users.

✉ Toshikazu Ushijima  
tushijim@ncc.go.jp

<sup>1</sup> Division of Epigenomics, National Cancer Center Research Institute, Tokyo, Japan

<sup>2</sup> Course of Advanced Clinical Research of Cancer, Juntendo University Graduate School of Medicine, Tokyo, Japan

<sup>3</sup> Department of Gastroenterology and Gastrointestinal Oncology, National Cancer Center Hospital East, Chiba, Japan

<sup>4</sup> Central Animal Division, National Cancer Center Research Institute, 5-1-1 Tsukiji, Chuo-ku, Tokyo 104-0045, Japan

<sup>5</sup> Department of Surgical Oncology, Osaka City University Graduate School of Medicine, Osaka, Japan

## Introduction

Cancer is caused by irreversible changes of gene function, namely genetic and epigenetic alterations [1]. Between these two kinds of alterations, gastric cancer is more heavily influenced by epigenetic alterations, namely aberrant DNA methylation [2–4]. Analysis of the mutation and methylation burdens in gastric tissues demonstrated that the accumulation of aberrant DNA methylation has a 2.3-fold stronger impact on gastric cancer risk than that of point mutations [3]. In addition, a multicenter prospective cohort study demonstrated that even among gastric cancer patients treated by endoscopic submucosal dissection, DNA methylation accumulation in gastric mucosa can predict the risk of metachronous gastric cancer [5, 6]. Furthermore, the simultaneous analysis of genetic and epigenetic alterations in gastric cancer has shown that major cancer-related pathways are affected more

frequently by aberrant DNA methylation than by genetic alterations [7].

To remove aberrant DNA methylation, DNA demethylating agents, such as 5-aza-2'-deoxycytidine (5-aza-dC) and 5-azacytidine (5-aza-CR), are approved by the US Food and Drug Administration, and clinically used for the treatment of myelodysplastic syndromes (MDS) and acute myeloid leukemia (AML) [8–10]. Multiple clinical trials involving the treatment of solid tumors with a DNA demethylating agent are currently being conducted. Some trials have shown promising results by restoring drug sensitivity to lung and ovarian cancers that were once resistant to cytotoxic drugs [11, 12]. This method is known as epigenetic priming [13, 14]. The use of a DNA demethylating agent may be useful for the treatment of gastric cancers, considering the limited number of molecular target drugs available [15–17] and the limited efficacy of the immune-check point inhibitors [18–20]. A recent phase I study on epigenetic priming using 5-aza-CR in gastric cancer showed that the priming in combination with epirubicin, oxaliplatin, and capecitabine (EOX) was well tolerated in a neoadjuvant setting and that some of the six loci analyzed were successfully demethylated by the priming [21]. However, priming effect for the other key cytotoxic drugs of gastric cancer, such as irinotecan and taxane, has not been examined, and, importantly, the mechanisms of how epigenetic priming works are still unclear.

In this study, we aimed to investigate which clinically used cytotoxic drugs can be effectively administered in combination with epigenetic priming and how epigenetic priming works in gastric cancer.

## Materials and methods

### Chemicals

Four chemotherapeutic drugs, namely, SN38 (the active metabolite of irinotecan), cisplatin (CDDP), paclitaxel (PTX; a taxane), and 5-fluorouracil (5-FU), and a demethylating agent, 5-aza-2'-deoxycytidine (5-aza-dC) were purchased from Sigma-Aldrich (St. Louis, MO, USA). SN38 and 5-FU were dissolved in dimethyl sulfoxide (DMSO). CDDP, PTX, and 5-aza-dC were dissolved in phosphate buffered saline (PBS).

### Gastric cancer cell lines

MKN45 and NUGC3 cell lines were purchased from the Japanese Collection of Research Bioresources (Tokyo, Japan), MKN1 cell line from RIKEN BioResource Center Cell Bank (Tsukuba, Japan), and AGS cell line from the American Type Culture Collection (ATCC; Manassas, VA, USA).

44As3, HSC43, and HSC60 cell lines were kindly provided by Dr. K. Yanagihara at the National Cancer Center, and TMK1 cell line by Dr. W. Yasui at Hiroshima University. The OCUM-2 M/SN38 cell line was established as an SN38-resistant cell line from OCUM-2M [22]. The cells were cultured in Roswell Park Memorial Institute (RPMI)-1640 (MKN45, NUGC3, AGS, 44As3, HSC43, HSC60, MKN1, and TMK1) or Dulbecco's modified Eagle medium (DMEM) with high glucose (OCUM-2M and OCUM-2M/SN38) at 37 °C in a humidified atmosphere with 5% CO<sub>2</sub>. All media were supplemented with 10% fetal bovine serum and 1% penicillin/streptomycin. The cells were tested for *Mycoplasma* infection using the MycoAlert mycoplasma detection kit (Lonza; Basel, Switzerland).

### Cell treatment and viability assay

For the sensitivity assay to cytotoxic drugs (Supplementary Fig. S1a), cells were seeded at a density of  $2 \times 10^3$  cells per well in a 96-well microplate on day 0 in triplicate. The cells were treated with a cytotoxic drug on day 1 for 72 h, and cell viability was evaluated using a WST-8 [2-(2-methoxy-4-nitrophenyl)-3-(4-nitrophenyl)-5-(2, 4-disulfophenyl)-2H tetrazolium, monosodium salt] assay (Nacalai Tesque Inc., Kyoto, Japan) on day 4. Briefly, each well in the 96-well plate was added with 10  $\mu$ l of WST-8 and incubated for 2 h at 37 °C. The absorbance of each sample was determined using a microplate reader (Wallac 1420 Victor2, Perkin-Elmer, Waltham, MA) with a reference wavelength of 450 nm. The average of the triplicate values was normalized against that of untreated cells. The half maximal inhibitory concentration (IC<sub>50</sub>) and a 95%-confidence interval were calculated by the non-linear regression analysis of log (inhibitor) versus the normalized response with a variable slope using a GraphPad Prism program (GraphPad Software, La Jolla, CA).

For the analysis of 5-aza-dC priming (Supplementary Fig. S1b), cells were seeded at a density of  $3 \times 10^4$  cells in a 10-cm dish on day 0 in triplicate. On days 1 to 3, cells were treated with 5-aza-dC (0.03  $\mu$ M for NUGC3, AGS, and 44As3; and 0.3  $\mu$ M for TMK1, OCUM-2 M, and OCUM-2 M/SN38). The medium was replaced on day 4, and the cells in the well were re-plated at a density of  $2 \times 10^3$  cells per well in the 96-well microplate on day 7. Different concentrations of chemotherapeutic drugs were administered on day 8 for 72 h (after 4 days of drug holiday). Cell viability was assessed on day 11 using a microplate reader as described above. The triplicate experiments were repeated thrice to evaluate biological fluctuations.

For the expression microarray analysis (Supplementary Fig. S1c), cells were seeded at a density of  $3 \times 10^4$  cells in a 10-cm dish on day 0. On day 1 to 3, cells were treated with 5-aza-dC (0.03  $\mu$ M for 44As3; 0.3  $\mu$ M for TMK1 and OCUM-2M/SN38), and the medium was replaced on day

4. The cells ( $4\text{--}6 \times 10^5$ ) were re-plated in a 10-cm dish on day 7. A cytotoxic drug was administered (SN38, 20 nM for 44As3 and OCUM-2 M/SN38; CDDP, 3  $\mu\text{M}$  for TMK1) on day 8 after 4 days of drug holiday, and RNA was extracted on day 9 to collect cells before death of responding cells.

For the DNA methylation analysis (Supplementary Fig. S1d), cells were seeded at  $3 \times 10^4$  cells in a 10-cm dish on day 0. On day 1 to 3, cells were treated with 5-aza-dC (0.1  $\mu\text{M}$  for 44As3; 0.3  $\mu\text{M}$  for OCUM-2 M/SN38 and TMK1), and the medium was replaced with fresh medium on day 4. DNA was extracted on day 8 (after 4 days of drug holiday) to obtain information of potentially primed cells.

### Expression microarray experiments and data processing

Total RNA was extracted using the ReliaPrep™ RNA Cell Miniprep System (Promega, Madison, WI, USA). Cy3-labeled cRNA was synthesized from 200 ng of total RNA using a Low Input Quick Amp Labeling Kit (Agilent Technologies, Santa Clara, CA, USA), and 600 ng of labeled cRNA was fragmented and hybridized to a gene expression microarray (SurePrint G3 Human Gene Expression  $8 \times 60$  K v2 Microarray; Agilent Technologies). The hybridized microarray was scanned with an Agilent G2565BA microarray scanner (Agilent Technologies). The scanned data were processed using Feature Extraction Ver.10.7 software (Agilent Technologies), and analyzed using GeneSpring Ver.13.5 software (Agilent Technologies). The 75th percentile of the signal intensity of all probes was normalized to be 0, and the signals were distributed from  $-7$  to 10. A signal intensity above  $-1$  was considered as positive expression. The expression microarray experiment was conducted once for a sample, based upon the high reproducibility reported [23].

### Ingenuity pathways analysis (IPA)

Analysis of the biological functions of the microarray data was performed using Ingenuity Pathway Analysis (IPA) (Qiagen, Ingenuity H Systems, Redwood City, CA; <http://www.ingenuity.com>). A gene set was prepared from the microarray data by selecting genes whose expression was induced ( $\geq 2$ -fold) by the 5-aza-dC priming and that were abundantly expressed (signal intensity  $> -1$ ). By performing the core analysis, the modules of “Diseases and Bio-functions” module were algorithmically generated from the gene set. The *P* values were calculated using a right-tailed Fisher’s exact test.

### Gene-specific expression analysis

cDNA was synthesized from 1  $\mu\text{g}$  of total RNA using reverse-transcriptase (SuperScript IV; Invitrogen, Carlsbad,

CA, USA). Quantitative PCR was carried out using SYBER Green I and specific primers to the individual genes. The amplification of a sample cDNA was compared to control samples with known copy numbers of target DNA, and the number of cDNA molecules was obtained. The number of the target gene was normalized to that of *GAPDH*. The primer sequences and PCR conditions are given in Supplementary Table 1.

### Genome-wide DNA methylation analysis

The genome-wide DNA methylation analysis was carried out using an Infinium HumanMethylation450 BeadChip array (Illumina, San Diego, CA, USA) as previously described [24]. The methylation levels of 485,512 probes (482,421 probes for CpG sites and 3,091 probes for non-CpG sites) were obtained as a  $\beta$  value that ranged from 0 (completely unmethylated) to 1 (completely methylated). The probes were assembled into 296,494 genomic blocks comprising one to multiple CpG sites (mean = 1.7) within 500 bp [25, 26]. The genomic blocks were classified based on their locations relative to a transcription start site (TSS) [TSS200 (200 bp upstream region from TSS), TSS1500 (regions between 200 bp upstream and 1,500 bp upstream from TSS), 5'-UTR, 1st exon, gene body, 3'-UTR, and intergenic region] and their locations against a CpG island (CGI) (N Shelf, N Shore, CGI, S Shore, S Shelf, and non-CGI). The methylation microarray experiment was conducted once for a sample, based upon the high reproducibility reported [27].

### Xenograft tumor formation assay in nude mice

OCUM-2 M/SN38 ( $1.0 \times 10^6$ ) cells were injected subcutaneously into the left flank of 6-week-old female nude mice (BALB/c-nu/nu; CLEA Japan, Tokyo, Japan). When tumors reached a volume of 200 mm<sup>3</sup>, the mice were randomized into four groups (7 mice per group); (1) vehicle (5% DMSO), (2) 5-aza-dC (2.5 mg/kg), (3) irinotecan (20 mg/kg), and (iv) both 5-aza-dC and irinotecan. 5-Aza-dC was intraperitoneally administered daily from days 1 to 3. After 3 days of drug holiday, irinotecan was intraperitoneally administered on day 7. The animal body weight and the length and width of the tumors were measured twice per week. The tumor volume was calculated using the following formula: (length  $\times$  width<sup>2</sup>)  $\times 0.5$ . After three courses of treatment (one course/week), tumors were excised from the surviving mice, and their weights were measured. Total blood was collected for determination of the number of leukocytes, erythrocytes and platelets. All of the animal experimental procedures conducted in the present study were approved by the Committee for Ethics in Animal Experimentation at the National Cancer Center.

## Immunohistochemistry

For the immunohistochemistry, four- $\mu\text{m}$  tissue sections were prepared from formalin fixed, paraffin-embedded blocks. Deparaffinized and rehydrated sections were incubated in HistoVT One (Nacalai Tesque) at 80 °C for 40 min to unmask the antigen [28]. After blocking with Blocking One Histo (Nacalai Tesque), the sections were stained with a rabbit anti-human Ki-67 antibody (Clone SP6; Thermo Fisher Scientific, Fremont, CA, USA) with 500-fold dilution at 4 °C overnight. The immune complex was visualized using a Vectastain Elite ABC kit (Vector Laboratories, Burlingame, CA, USA). Microscopic images were obtained using a BZ-X710 microscope system (Keyence, Osaka, Japan). To analyze the number of the positive cells, cells were counted in three randomly selected areas. The Ki-67 labeling index was defined as a percentage of the positive cells in the number of counted cells (the mean of the counted cells: mock, 1,119 cells/area; 5-aza-dC, 776 cells/area; irinotecan, 686 cells/area; and 5-aza-dC + irinotecan, 862 cells/area).

## Results

### Identification of gastric cancer cell lines resistant to chemotherapeutic drugs in clinical use

To identify the gastric cancer cell lines resistant to chemotherapeutic drugs in clinical use (SN38, CDDP, PTX, and 5-FU), we evaluated the drug sensitivity of ten gastric cancer cell lines (Fig. 1a), and selected the two most resistant ones. For SN38, the  $\text{IC}_{50}$  values ranged from 2.4 to 44.1 nM, and TMK1 ( $\text{IC}_{50}=44.1$  nM) and 44As3 ( $\text{IC}_{50}=41.1$  nM) were selected as SN38-resistant cell lines. OCUM-2 M/SN38 was established as an SN38-resistant cell line ( $\text{IC}_{50}=31.1$  nM), and was also selected. For CDDP, the  $\text{IC}_{50}$  values ranged from 0.3 to 7.7  $\mu\text{M}$ , and TMK1 ( $\text{IC}_{50}=5.0$   $\mu\text{M}$ ) and OCUM-2 M ( $\text{IC}_{50}=6.0$   $\mu\text{M}$ ) were selected as CDDP-resistant cell lines. For 5-FU, the  $\text{IC}_{50}$  values ranged from 3.1 to 32.0  $\mu\text{M}$ , and TMK1 ( $\text{IC}_{50}=32.0$   $\mu\text{M}$ ) and NUGC3 ( $\text{IC}_{50}=21.1$   $\mu\text{M}$ ) were selected as 5-FU-resistant cell lines. For PTX, the  $\text{IC}_{50}$  values ranged from 1.5 to 10.9 nM, and TMK1 ( $\text{IC}_{50}=4.7$  nM) and AGS ( $\text{IC}_{50}=10.9$  nM) were selected as PTX-resistant cell lines (Fig. 1b).

### Enhancement of cytotoxic effect by epigenetic priming

To analyze the effect of epigenetic priming with 5-aza-dC, we evaluated changes in the sensitivity of the above mentioned cell lines after priming. To obtain the maximum demethylating effect by 5-aza-dC, we adopted a long-term

and low-dose protocol based on previously reported methods [29–31]. Among the four cytotoxic drugs, the effects of epigenetic priming were most pronounced on the cytotoxic effects of SN38 and CDDP, but not those of PTX and 5-FU (Fig. 2). Epigenetic priming lowered the  $\text{IC}_{50}$  values for SN38 from 226.4 to 32.9 nM (7-fold improvement) in TMK1, from 125.2 to 21.0 nM (6-fold) in 44As3, and from 73.4 to 16.5 nM (4-fold) in OCUM-2M/SN38. In addition, epigenetic priming also lowered the  $\text{IC}_{50}$  values for CDDP from 6.0 to 2.3  $\mu\text{M}$  (3-fold) in TMK1 and from 10.8 to 2.8  $\mu\text{M}$  (4-fold) in OCUM-2 M.

### Reactivated pathways by the epigenetic priming

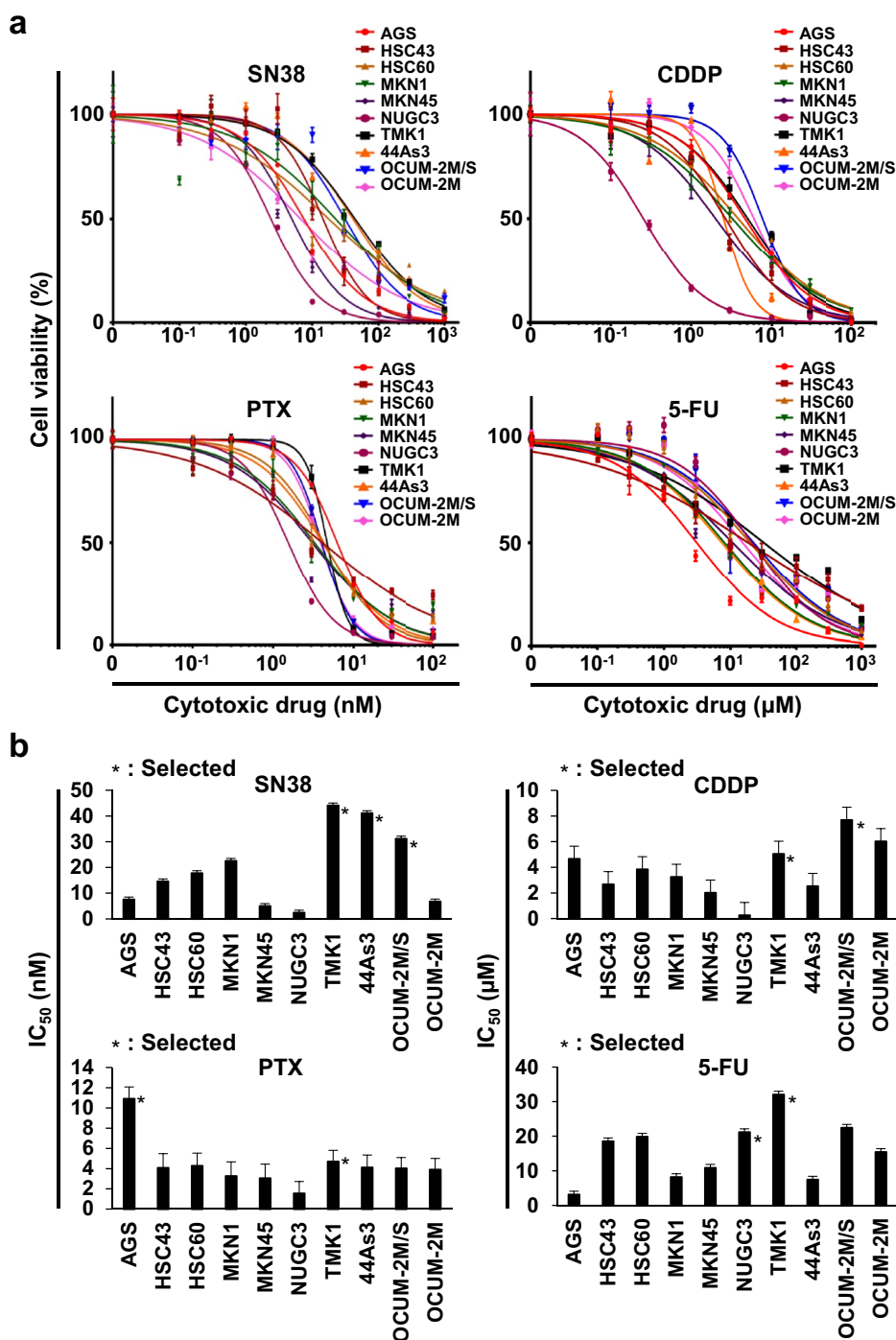
To investigate the mechanisms of how the epigenetic priming enhanced the cytotoxic effects of SN38 and CDDP in their resistant cell lines, we analyzed the gene expression profiles using microarrays. Among the three cell lines treated with SN38, 44As3 and OCUM-2 M/SN38 were selected. Among the two cell lines treated with CDDP, TMK1 was selected. Using the three cell lines, gene expression profiles were obtained from the following four treatment groups: (i) mock-treated cells, (ii) cells treated with a cytotoxic drug only, (iii) cells treated with epigenetic priming only, (iv) cells treated with a cytotoxic drug after epigenetic priming.

The biological functions of the up-regulated genes in (iv) cells treated with a cytotoxic drug after epigenetic priming compared with (i) mock-treated cells were screened by IPA. The cell death and survival category was one of the top five significantly enriched categories in the molecular and cellular functional categories of the “Disease and Bio-Functions” module (Fig. 3a). Notably, this biological function was selected based on IPA of all three cell lines. Furthermore, characteristics of the annotated genes in the cell death and survival category were examined, and five genes associated with apoptosis and cell death (*RUNX3*, *PYCARD*, *TNF*, *FAS*, and *FASLG*) were identified from the cell death and survival category.

To confirm the expression changes in the isolated genes, quantitative RT-PCR was performed. The isolated genes were expressed at considerably higher levels in cells with epigenetic priming than in those without priming (Fig. 3b). Of note, cytotoxic drug treatment only did not upregulate these genes, but epigenetic priming reactivated these genes (in 44As3 and TNK1). Even in OCUM-2M/SN38 with established SN38 resistance, epigenetic priming activated genes associated with apoptosis and cell death after SN38 treatment. These results indicated that the apoptosis- and cell death-related genes were associated with the enhancement of the cytotoxic effects mediated by epigenetic priming.



**Fig. 1** Sensitivity of 10 gastric cancer cell lines to four clinically used cytotoxic drugs. **a** Dose–response curves of the 10 gastric cancer cell lines to SN38, CDDP, PTX, and 5-FU. Data are shown as the Mean  $\pm$  SEM obtained from three independent experiments. **b** The  $IC_{50}$  values of the 10 gastric cancer cell lines for individual drugs. The two (three for SN38) most resistant cell lines (shown by asterisks) were selected and used for the following experiments

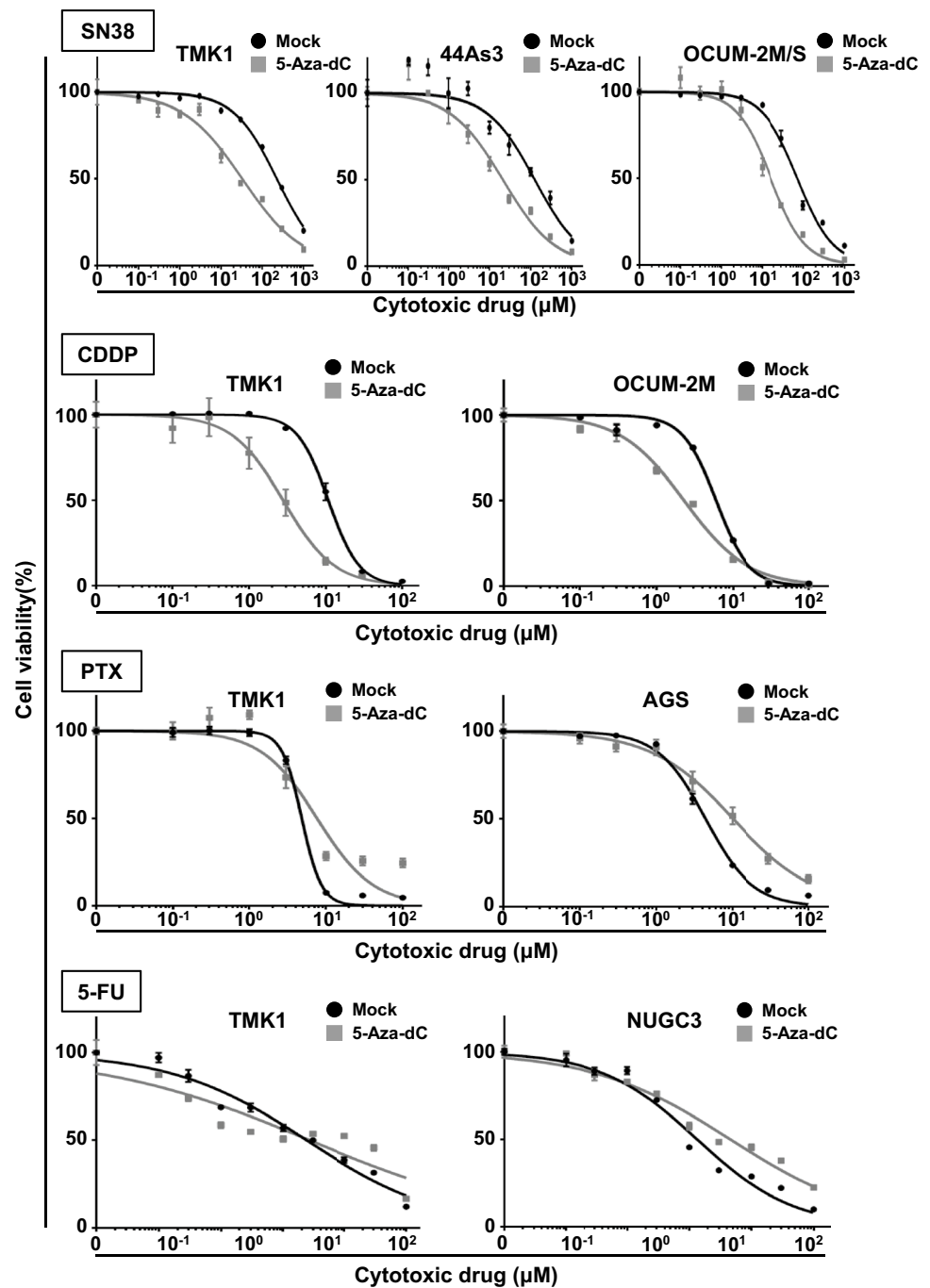


## Methylation changes underlying the reactivated genes

To investigate whether the reactivation was caused by the demethylation effect of 5-aza-dC, we explored the methylation status of the reactivated genes. In all three cell lines, extensive global demethylation was observed in the cells subjected to epigenetic priming compared to that in non-treated cells in all three cell lines (Fig. 4a). Among the above

reactivated genes, the demethylation of the CpG island of the *RUNX3* promoter was evident (Fig. 4b). The CpG island of the *PYCARD* promoter was demethylated; however, it was only partially methylated even in non-treated cells. Given this outcome, it remains unclear whether the demethylation was responsible for gene reactivation. The *FAS* CpG island was not methylated even in non-treated cells. *FASLG* and *TNF* did not have promoter CpG islands, and the effect of demethylation on transcription remains unclear.

**Fig. 2** Effect of epigenetic priming by 5-aza-dC. Resistant cells were first treated with 5-aza-dC or mock first, and subsequently treated with a cytotoxic drug. The  $IC_{50}$  values were significantly lower for SN38 and CDDP, but not for PTX and 5-FU



### In vivo tumor suppression effect of epigenetic priming

Finally, the in vivo effects of epigenetic priming were analyzed using an OCUM-2 M/SN38 xenograft model, which is well known as a model of SN38 resistance [22]. The administration of 5-aza-dC exerted weak tumor suppression effects, and irinotecan treatment showed only moderate tumor suppression effects (Fig. 5a, b, and c). However, after the epigenetic priming, irinotecan showed strong tumor

suppression effects. Histologically, both 5-aza-dC and irinotecan treatment induced cell loss, and 5-aza-dC treatment additionally accentuated diverse cellular morphology, including cellular enlargement, nuclear swelling, and cytoplasmic degeneration, including pseudoground glass appearance or vacuolization (Fig. 5d). The irinotecan treatment after epigenetic priming induced massive cell loss with fibrosis and inflammation, and enlarged cells constituted the major the surviving cells. The Ki-67 immunohistochemistry showed that the number of Ki-67-positive cells was

**Fig. 3** Identification of pathways and genes reactivated by epigenetic priming. Genes up-regulated by the epigenetic priming and drug treatment were identified by expression microarray in 44As3 and OCUM-2 M/SN38 for SN38, and in TMK1 for CDDP. **a** IPA analysis of the biological functions of the up-regulated genes during treatment. The cell death and survival category was one of the top five most significantly enriched functions. **b** Confirmation of the expression of five genes associated with apoptosis and cell death (*RUNX3*, *TNF*, *PYCARD*, *FAS*, and *FASLG*) by quantitative RT-PCR

	Molecular and Cellular Top 5 Functions	P-Value
<b>44As3</b>	1 Cellular Movement	8.29E-06 to 1.16E-21
	2 Cell-To-Cell Signaling and Interaction	7.57E-06 to 1.44E-13
	3 Cellular Function and Maintenance	8.46E-06 to 5.13E-13
	4 Cell Death and Survival	7.95E-06 to 2.08E-12
	5 Cellular Development	8.15E-06 to 2.38E-12
<b>OCUM-2M/S</b>	1 Cellular Movement	9.88E-04 to 3.46E-14
	2 Cell Death and Survival	1.15E-03 to 4.22E-08
	3 Lipid Metabolism	9.88E-04 to 2.67E-07
	4 Small Molecule Biochemistry	9.88E-04 to 2.67E-07
	5 Cell Signaling	8.46E-04 to 5.09E-07
<b>TMK1</b>	1 Cellular Movement	1.29E-06 to 5.06E-26
	2 Cell Death and Survival	1.62E-06 to 3.66E-20
	3 Cellular Growth and Proliferation	1.66E-06 to 2.88E-17
	4 Cellular Development	1.66E-06 to 3.59E-17
	5 Cellular Function and Maintenance	1.57E-06 to 5.93E-16

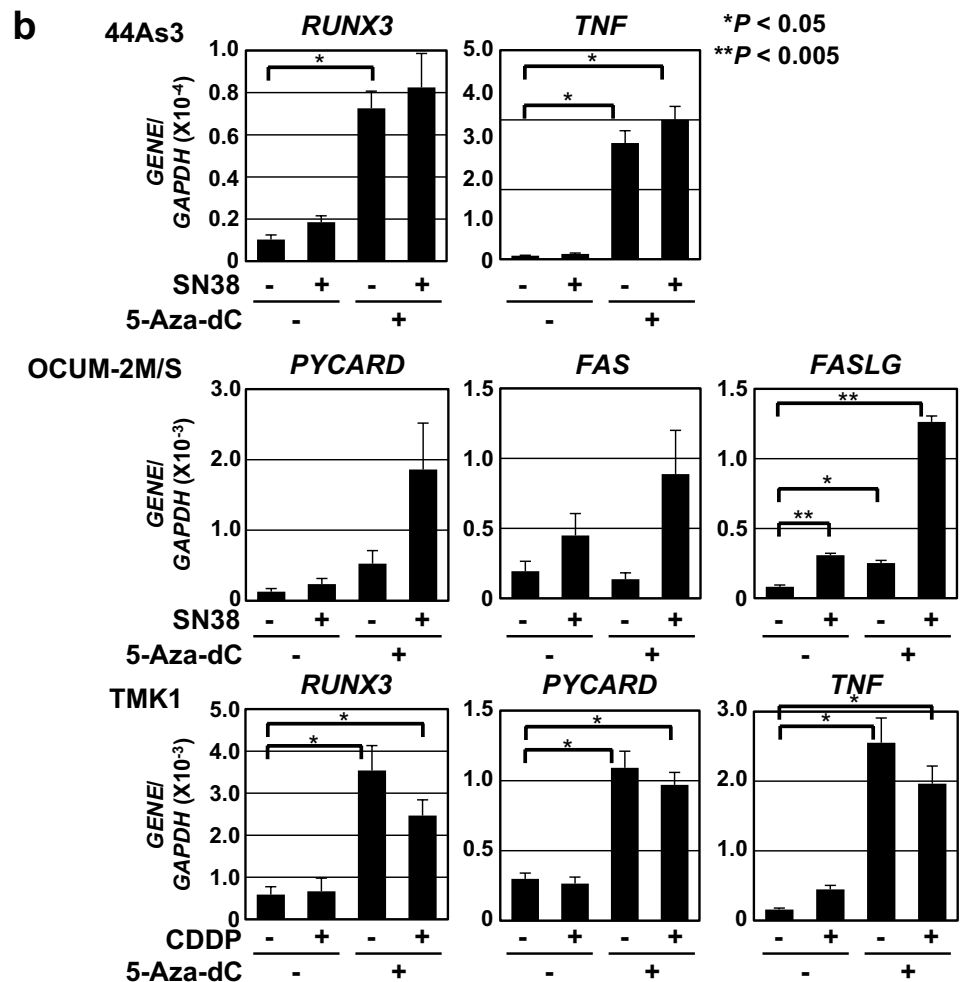
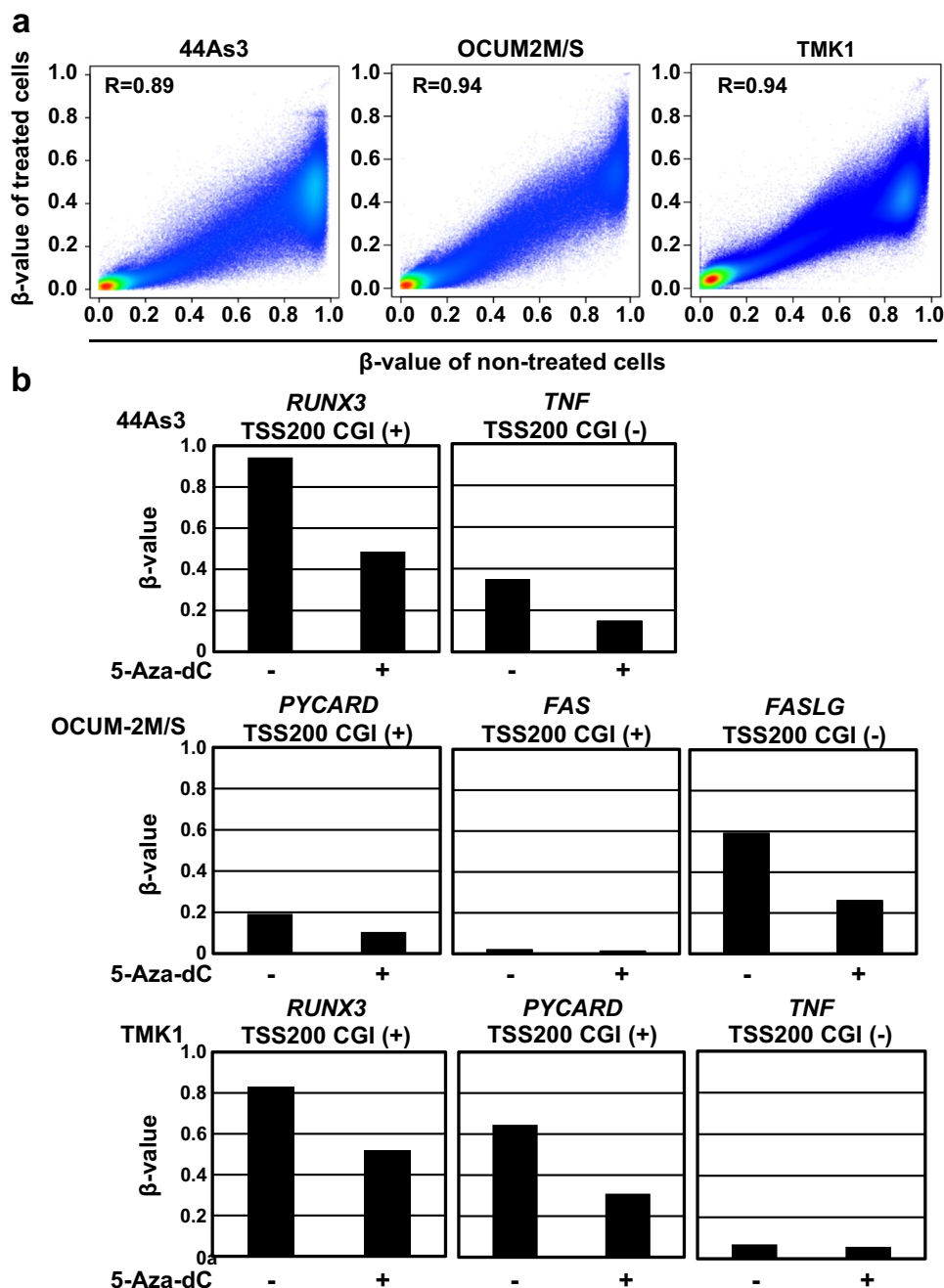


**Fig. 4** DNA methylation analysis by DNA methylation microarray. **a** Extensive DNA demethylation by epigenetic priming. **b** Demethylation of *RUNX3* and *PYCARD* promoter CGI. *FAS* has a promoter CGI, but was not methylated in cancer cells. *FASLG* and *TNF* do not have promoter CGIs and were unlikely to be methylation-silenced



significantly decreased by irinotecan treatment or epigenetic priming, and was significantly decreased by irinotecan treatment after epigenetic priming (Fig. 5e, f).

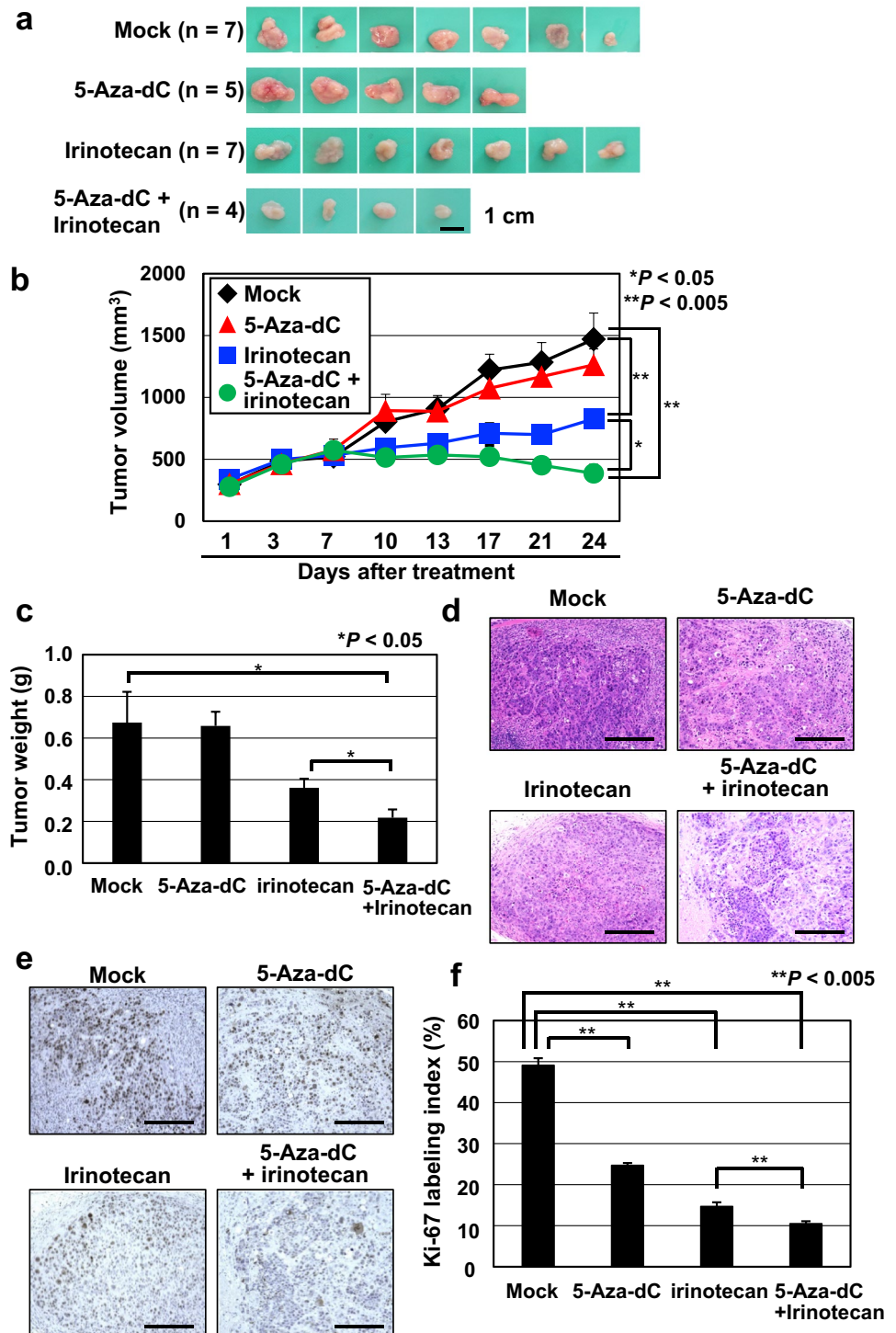
Regarding the adverse effects of the treatment, body weight loss was observed in mice treated with 5-aza-dC (Supplementary Fig. S2a), but the body weights were recovered after termination of the treatment. Notably, two of the seven mice in the 5-aza-dC group and three of the seven epigenetic priming group died before 24 days; three of the five mice showed body weight loss, but the causes of death of the remaining two were unclear. Severe hematotoxicity was observed in mice

treated with 5-aza-dC (Supplementary Fig. S2b). These results showed that 5-aza-dC priming enhanced the cytotoxic effects of irinotecan treatment in vivo and that the adverse effects need to be reduced by a further dose adjustment of 5-aza-dC priming.



**Fig. 5** In vivo effect of epigenetic priming on the resistance of OCUM-2 M/SN38 to SN38.

**a** Macroscopic view of the xenografts in the four treatment groups. **b** Tumor growth curves of the four treatment groups. Although only irinotecan showed a growth-suppressive effect, this was augmented by epigenetic priming. **c** The therapeutic effect assessed by tumor weight at necropsy. **d** Representative HE staining in the four treatment groups. **e** Ki-67 immunohistochemistry in the four treatment groups. **f** Ki-67 labeling index in the four treatment groups



## Discussion

Epigenetic priming was shown to be effective for SN38, an active metabolite of irinotecan, and for CDDP in gastric cancer cell lines. The reactivation of genes involved in the cell death and survival category was shown mechanistically, and the demethylation of the promoter CpG islands of at least

*RUNX3*, and possibly *PYCARD*, was identified. *RUNX3* is a well-known tumor-suppressor gene in gastric cancer that plays pleiotropic functions, such as cell cycle regulation in cooperation with p53 and augmentation of the tumor-suppressive activity of TGF- $\beta$  [32, 33]. *PYCARD*, also known as *ASC* or *TMS1*, is involved in the regulation of apoptosis and the inflammasome [34]. Even in vivo, the priming

effect of a DNA demethylating agent for irinotecan was also shown. The results provided a rationale for conducting further preclinical studies to implement epigenetic priming prior to standard therapy for gastric cancer. Genes in the “cell movement category” were consistently up-regulated, and this was due to up-regulation of immune-related genes, such as *IL1 $\beta$*  and *IL32*.

We tested four key cytotoxic drugs for gastric cancer treatment, namely SN38, CDDP, PTX, and 5-FU, as potential combination partners for epigenetic priming using the cell lines that were most resistant to the individual drugs. As a result, the priming effects were evident for SN38 and CDDP, but not for PTX and 5-FU. The epigenetic priming activated genes involved in apoptosis and cell death, such as *RUNX3*, *TNF*, *PYCARD*, *FAS*, and *FASLG*. Few reports are available for the direct involvement of their inactivation in SN38 or CDDP resistance, and involvement via apoptosis suppression was suggested. Indeed, in ovarian cancer, the up-regulation of genes involved in DNA repair and antitumor immune responses has been reported to mediate enhanced CDDP sensitivity [35]. In colon cancer, the re-expression of genes involved in cell adhesion and DNA repair has been reported to enhance irinotecan sensitivity [36].

The regulation of *RUNX3* by DNA methylation was indicated in 44As3 and TMK1, and that of *PYCARD* was suggested in TMK1. In contrast, although *TNF* was strongly induced by epigenetic priming in 44As3 and TMK1, it is unlikely to be regulated by DNA methylation, since *TNF* does not have a promoter CGI. Nevertheless, TNF could serve as an important mediator of epigenetic priming. TNF is well established to be capable of inducing apoptosis [37], and its transcription is controlled by multiple transcription factors [38]. There is a possibility that the methylation-silencing of such transcription factors or their co-factors was restored by epigenetic priming.

In vivo experiments also showed the effect of epigenetic priming effect for irinotecan. However, the dose and schedule adopted here caused severe leukopenia (Supplementary Fig. S2b). The dose of 2.5 mg/kg and schedule of three consecutive days were determined based on previous reports [30]. However, since the priming effect was sufficiently observed, there seems to be room for reducing the dose or days of administration. The death of two and three mice in the 5-aza-dC and epigenetic priming groups, respectively, also indicated the need for dose reduction. Since it is known that the maximum biological dose, not the maximum tolerated dose, is important for epigenetic therapy, we need to explore the dose and schedule that produces the maximum DNA demethylation effect in tumor cells and the least cytotoxic effects in bone marrow cells.

In conclusion, epigenetic priming was found to be effective for gastric cancer cell lines that are resistant to SN38 and CDDP. In addition, our results indicated that epigenetic

priming is primarily mediated by the activation of apoptosis- and cell death-related genes.

**Funding** This study was supported by AMED under grant number JP19ck0106421.

## Compliance with ethical standards

**Conflicts of interest** T. U. has received a research grant from Ohara Pharmaceutical Co, Ltd. The other authors declare that they have no conflict of interest.

**Ethical approval** All institutional and national guidelines for the care and use of laboratory animals were followed.

## References

1. Jones PA, Issa JP, Baylin S. Targeting the cancer epigenome for therapy. *Nat Rev Genet.* 2016;17:630–41.
2. Ushijima T, Sasako M. Focus on gastric cancer. *Cancer Cell.* 2004;5:121–5.
3. Yamashita S, Kishino T, Takahashi T, Shimazu T, Charvat H, Kakugawa Y, et al. Genetic and epigenetic alterations in normal tissues have differential impacts on cancer risk among tissues. *Proc Natl Acad Sci USA.* 2018;115:1328–33.
4. Toyota M, Ahuja N, Suzuki H, Itoh F, Ohe-Toyota M, Imai K, et al. Aberrant methylation in gastric cancer associated with the CpG island methylator phenotype. *Cancer Res.* 1999;59:5438–42.
5. Asada K, Nakajima T, Shimazu T, Yamamichi N, Maekita T, Yokoi C, et al. Demonstration of the usefulness of epigenetic cancer risk prediction by a multicentre prospective cohort study. *Gut.* 2015;64:388–96.
6. Maeda M, Nakajima T, Oda I, Shimazu T, Yamamichi N, Maekita T, et al. High impact of methylation accumulation on metachronous gastric cancer: 5-year follow-up of a multicentre prospective cohort study. *Gut.* 2017;66:1721–3.
7. Yoda Y, Takeshima H, Niwa T, Kim JG, Ando T, Kushima R, et al. Integrated analysis of cancer-related pathways affected by genetic and epigenetic alterations in gastric cancer. *Gastric Cancer.* 2015;18:65–76.
8. Kantarjian H, Issa JP, Rosenfeld CS, Bennett JM, Albitar M, DiPersio J, et al. Decitabine improves patient outcomes in myelodysplastic syndromes: results of a phase III randomized study. *Cancer.* 2006;106:1794–803.
9. Diesch J, Zwick A, Garz AK, Palau A, Buschbeck M, Gotze KS. A clinical-molecular update on azanucleoside-based therapy for the treatment of hematologic cancers. *Clin Epigenetics.* 2016;8:71.
10. Stresemann C, Lyko F. Modes of action of the DNA methyltransferase inhibitors azacytidine and decitabine. *Int J Cancer.* 2008;123:8–13.
11. Juergens RA, Wrangle J, Vendetti FP, Murphy SC, Zhao M, Coleman B, et al. Combination epigenetic therapy has efficacy in patients with refractory advanced non-small cell lung cancer. *Cancer Discov.* 2011;1:598–607.
12. Matei D, Fang F, Shen C, Schilder J, Arnold A, Zeng Y, et al. Epigenetic resensitization to platinum in ovarian cancer. *Cancer Res.* 2012;72:2197–205.
13. Scandura JM, Roboz GJ, Moh M, Morawa E, Brenet F, Bose JR, et al. Phase I study of epigenetic priming with decitabine prior to standard induction chemotherapy for patients with AML. *Blood.* 2011;118:1472–80.

14. Halpern AB, Othus M, Huebner EM, Buckley SA, Pogosova-Agadjanyan EL, Orlowski KF, et al. Mitoxantrone, etoposide and cytarabine following epigenetic priming with decitabine in adults with relapsed/refractory acute myeloid leukemia or other high-grade myeloid neoplasms: a phase 1/2 study. *Leukemia*. 2017;31:2560–7.
15. Bang YJ, Van Cutsem E, Feyereislova A, Chung HC, Shen L, Sawaki A, et al. Trastuzumab in combination with chemotherapy versus chemotherapy alone for treatment of HER2-positive advanced gastric or gastro-oesophageal junction cancer (ToGA): a phase 3, open-label, randomised controlled trial. *Lancet*. 2010;376:687–97.
16. Wilke H, Muro K, Van Cutsem E, Oh SC, Bodoky G, Shimada Y, et al. Ramucirumab plus paclitaxel versus placebo plus paclitaxel in patients with previously treated advanced gastric or gastro-oesophageal junction adenocarcinoma (RAINBOW): a double-blind, randomised phase 3 trial. *Lancet Oncol*. 2014;15:1224–35.
17. Cancer Genome Atlas Research Network. Comprehensive molecular characterization of gastric adenocarcinoma. *Nature*. 2014;513:202–9.
18. Kang YK, Boku N, Satoh T, Ryu MH, Chao Y, Kato K, et al. Nivolumab in patients with advanced gastric or gastro-oesophageal junction cancer refractory to, or intolerant of, at least two previous chemotherapy regimens (ONO-4538-12, ATTRACTION-2): a randomised, double-blind, placebo-controlled, phase 3 trial. *Lancet*. 2017;390:2461–71.
19. Shitara K, Ozguroglu M, Bang YJ, Di Bartolomeo M, Mandala M, Ryu MH, et al. Pembrolizumab versus paclitaxel for previously treated, advanced gastric or gastro-oesophageal junction cancer (KEYNOTE-061): a randomised, open-label, controlled, phase 3 trial. *Lancet*. 2018;392:123–33.
20. Kim ST, Cristescu R, Bass AJ, Kim KM, Odegaard JI, Kim K, et al. Comprehensive molecular characterization of clinical responses to PD-1 inhibition in metastatic gastric cancer. *Nat Med*. 2018;24:1449–58.
21. Schneider BJ, Shah MA, Klute K, Ocean A, Popa E, Altorki N, et al. Phase I study of epigenetic priming with azacitidine prior to standard neoadjuvant chemotherapy for patients with resectable gastric and esophageal adenocarcinoma: evidence of tumor hypomethylation as an indicator of major histopathologic response. *Clin Cancer Res*. 2017;23:2673–80.
22. Zhang X, Yashiro M, Qiu H, Nishii T, Matsuzaki T, Hirakawa K. Establishment and characterization of multidrug-resistant gastric cancer cell lines. *Anticancer Res*. 2010;30:915–21.
23. Shi L, Reid LH, Jones WD, Shippy R, Warrington JA, Baker SC, et al. The MicroArray Quality Control (MAQC) project shows inter- and intraplatform reproducibility of gene expression measurements. *Nat Biotechnol*. 2006;24:1151–61.
24. Shigematsu Y, Niwa T, Yamashita S, Taniguchi H, Kushima R, Katai H, et al. Identification of a DNA methylation marker that detects the presence of lymph node metastases of gastric cancers. *Oncol Lett*. 2012;4:268–74.
25. Iida N, Okuda Y, Ogasawara O, Yamashita S, Takeshima H, Ushijima T. MACON: a web tool for computing DNA methylation data obtained by the Illumina Infinium Human DNA methylation BeadArray. *Epigenomics*. 2018;10:249–58.
26. Kim JG, Takeshima H, Niwa T, Rehnberg E, Shigematsu Y, Yoda Y, et al. Comprehensive DNA methylation and extensive mutation analyses reveal an association between the CpG island methylator phenotype and oncogenic mutations in gastric cancers. *Cancer Lett*. 2013;330:33–40.
27. Bibikova M, Barnes B, Tsan C, Ho V, Klotzle B, Le JM, et al. High density DNA methylation array with single CpG site resolution. *Genomics*. 2011;98:288–95.
28. Hur K, Niwa T, Toyoda T, Tsukamoto T, Tatematsu M, Yang HK, et al. Insufficient role of cell proliferation in aberrant DNA methylation induction and involvement of specific types of inflammation. *Carcinogenesis*. 2011;32:35–41.
29. Tsai HC, Li H, Van Neste L, Cai Y, Robert C, Rassool FV, et al. Transient low doses of DNA-demethylating agents exert durable antitumor effects on hematological and epithelial tumor cells. *Cancer Cell*. 2012;21:430–46.
30. Zong L, Hattori N, Yasukawa Y, Kimura K, Mori A, Seto Y, et al. LINC00162 confers sensitivity to 5-Aza-2'-deoxycytidine via modulation of an RNA splicing protein, HNRNPH1. *Oncogene*. 2019;38:5281–93.
31. Cui Y, Hausheer F, Beatty R, Zahnow C, Issa JP, Bunz F, et al. A recombinant reporter system for monitoring reactivation of an endogenously DNA hypermethylated gene. *Cancer Res*. 2014;74:3834–43.
32. Chuang LS, Ito K, Ito Y. RUNX family: regulation and diversification of roles through interacting proteins. *Int J Cancer*. 2013;132:1260–71.
33. Bae SC, Kolinjivadi AM, Ito Y. Functional relationship between p53 and RUNX proteins. *J Mol Cell Biol*. 2018;11:224–30.
34. Salminen A, Kauppinen A, Hiltunen M, Kaarniranta K. Epigenetic regulation of ASC/TMS1 expression: potential role in apoptosis and inflammasome function. *Cell Mol Life Sci*. 2014;71:1855–64.
35. Fang F, Cardenas H, Huang H, Jiang G, Perkins SM, Zhang C, et al. Genomic and epigenomic signatures in ovarian cancer associated with resensitization to platinum drugs. *Cancer Res*. 2018;78:631–44.
36. Sharma A, Vata-palli R, Abdelfatah E, Wyatt McMahon K, Kerner Z, Guzzetta AA, et al. Hypomethylating agents synergize with irinotecan to improve response to chemotherapy in colorectal cancer cells. *PLoS One*. 2017;12:e0176139.
37. Annibaldi A, Meier P. Checkpoints in TNF-induced cell death: implications in inflammation and cancer. *Trends Mol Med*. 2018;24:49–65.
38. Falvo JV, Tsytsykova AV, Goldfeld AE. Transcriptional control of the TNF gene. *Curr Dir Autoimmun*. 2010;11:27–60.

**Publisher's Note** Springer Nature remains neutral with regard to jurisdictional claims in published maps and institutional affiliations.